

ARTICLE OPEN



Nek2A prevents centrosome clustering and induces cell death in cancer cells via KIF2C interaction

Batuhan Mert Kalkan^{1,2}, Selahattin Can Ozcan², Enes Cicek^{1,2}, Mehmet Gonen^{3,4} and Ceyda Acilan^{2,3}✉

© The Author(s) 2024

Unlike normal cells, cancer cells frequently exhibit supernumerary centrosomes, leading to formation of multipolar spindles that can trigger cell death. Nevertheless, cancer cells with supernumerary centrosomes escape the deadly consequences of unequal segregation of genomic material by coalescing their centrosomes into two poles. This unique trait of cancer cells presents a promising target for cancer therapy, focusing on selectively attacking cells with supernumerary centrosomes. Nek2A is a kinase involved in mitotic regulation, including the centrosome cycle, where it phosphorylates linker proteins to separate centrosomes. In this study, we investigated if Nek2A also prevents clustering of supernumerary centrosomes, akin to its separation function. Reduction of Nek2A activity, achieved through knockout, silencing, or inhibition, promotes centrosome clustering, whereas its overexpression results in inhibition of clustering. Significantly, prevention of centrosome clustering induces cell death, but only in cancer cells with supernumerary centrosomes, both in vitro and in vivo. Notably, none of the known centrosomal (e.g., CNAP1, Rootletin, Gas2L1) or non-centrosomal (e.g., TRF1, HEC1) Nek2A targets were implicated in this machinery. Additionally, Nek2A operated via a pathway distinct from other proteins involved in centrosome clustering mechanisms, like HSET and NuMA. Through TurboID proximity labeling analysis, we identified novel proteins associated with the centrosome or microtubules, expanding the known interaction partners of Nek2A. KIF2C, in particular, emerged as a novel interactor, confirmed through coimmunoprecipitation and localization analysis. The silencing of KIF2C diminished the impact of Nek2A on centrosome clustering and rescued cell viability. Additionally, elevated Nek2A levels were indicative of better patient outcomes, specifically in those predicted to have excess centrosomes. Therefore, while Nek2A is a proposed target, its use must be specifically adapted to the broader cellular context, especially considering centrosome amplification. Discovering partners such as KIF2C offers fresh insights into cancer biology and new possibilities for targeted treatment.

Cell Death and Disease (2024)15:222; <https://doi.org/10.1038/s41419-024-06601-0>

INTRODUCTION

Centrosomes are key to microtubule organization and cell division, with their dysfunction linked to diseases like cancer, where cells often have excess centrosomes that promote genomic instability and tumor growth [1–3]. For cancer cells with supernumerary centrosomes, clustering is crucial to achieve bipolar division and sustain their survival. This process enables the formation of a functional bipolar spindle in mitosis, averting the emergence of lethal multipolar spindles. Hence, understanding the processes that govern centrosome clustering is vital to pinpoint new therapeutic strategies aimed at disrupting this clustering, offering a selective means to eliminate cancer cells.

One of the major regulators that control the centrosome cycle and separation is Nek2A kinase [4, 5]. Nek2A orchestrates centrosome separation by phosphorylating centrosomal linker proteins, such as C-Nap1 and rootletin, leading to their disassembly at the onset of mitosis [6–8]. This phosphorylation event weakens the cohesion between centrosomes, allowing them to move apart and form the poles of the mitotic spindle, which is crucial for proper chromosome segregation. Although the

role of Nek2A in centrosome separation is well-documented, it was unclear if similar mechanisms apply to the disjunction of supernumerary centrosomes and if Nek2A could interfere with centrosome clustering.

In this study, we investigated the potential of Nek2A to regulate clustering of centrosomes in cancer cells with supernumerary centrosomes, and whether impeding Nek2A-mediated prevention of centrosome clustering could emerge as a potential cancer treatment strategy. Our findings showed that while Nek2A overexpression could indeed interfere centrosome clustering, none of its known targets appeared to be involved in this process. Through proximity labelling, we identified a novel collaboration between Nek2A and KIF2C, a kinesin family member, that orchestrates centrosome clustering through a mechanism independent from those described earlier. Specifically, we found that KIF2C is indispensable for the prevention of clustering, triggered by Nek2A, a phenomenon exclusive to cancer cells with supernumerary centrosomes. We demonstrated that targeting cells with supernumerary centrosomes and elevated Nek2A/KIF2C expression could selectively kill cancer cells, a finding

¹Koç University, Graduate School of Health Sciences, Istanbul, Turkey. ²Koç University, Research Center for Translational Medicine, Istanbul, Turkey. ³Koç University, School of Medicine, Istanbul, Turkey. ⁴Koç University, College of Engineering, Department of Industrial Engineering, Istanbul, Turkey. ✉email: cayhan@ku.edu.tr
Edited by Professor Mauro Piacentini

Received: 24 November 2023 Revised: 5 March 2024 Accepted: 7 March 2024

Published online: 16 March 2024

substantiated both in vitro and in vivo. Moreover, in support of our hypothesis, high levels of Nek2A correlated with improved patient outcomes when centrosome amplification was predicted to be high.

RESULTS

Nek2A regulates centrosome clustering in cancer cells with supernumerary centrosomes

To evaluate Nek2A's role in centrosome clustering regulation, we generated a doxycycline (dox)-inducible lentiviral overexpression system. This was introduced into the N1E-115 mouse neuroblastoma cell line, known for its widespread supernumerary centrosomes and effective centrosome clustering (Supplementary Fig. 1A), making it an ideal model for study [9]. We stained the cells with DAPI, γ -Tubulin and α -Tubulin to determine the number of spindle poles and distinguish bipolar clustered and multipolar metaphases based on DNA shape and planar arrangement of centrosomes (Fig. 1A). Overexpression of Nek2A dramatically reduced centrosome clustering in N1E-115 cells, promoting formation of multipolar spindles (MPS) during metaphase (Fig. 1B, $p < 0.01$). In line with the hypothesis that centrosome clustering is vital for cancer cell survival, overexpression of Nek2A led to a marked reduction in cell viability in N1E-115 cells ($p < 0.001$). To determine if this observation isn't just specific to a particular cell line, we examined various human cancer cells, such as pancreatic ductal adenocarcinoma (PDAC), known for exhibiting centrosome amplification (CA) [10]. We characterised three PDAC cell lines (MIA PaCa-2, Panc1, and SU86.86) for PLK4 and STIL expressions, key indicators of CA (Supplementary Fig. 1B). Among three, SU86.86 showed the highest PLK4 levels and CA (~22%), confirmed by γ -Tubulin staining (Supplementary Fig. 1C, D). Hence, we generated a dox-inducible Nek2A overexpression in SU86.86 cells (Supplementary Fig. 1E) similar to N1E-115 and found that Nek2A significantly promoted MPS formation (Fig. 1C) and reduced cell viability (Fig. 1D), further implicating its role in averting centrosome clustering which trigger cell death.

Interestingly, during interphase, supernumerary centrosomes often appeared clustered together (Fig. 1E). Thus, we explored if Nek2A overexpression, which we found affects centrosome coalescence during mitosis, could also disperse these centrosomes in interphase. However, Nek2A did not alter the arrangement of supernumerary centrosomes in either N1E-115 or SU86.86 cells (Fig. 1F), suggesting that Nek2A's role in centrosome clustering is mitosis-dependent.

In order to test whether Nek2A can still regulate centrosome clustering in cells without amplification or low levels of CA, we overexpressed Nek2A in MDA-MB-231 (~7% CA) and U2OS cells (1% CA) (Supplementary Fig. 1F, G). Unlike cells with high CA and effective clustering, Nek2A overexpression did not intercept centrosome clustering in these cells (Supplementary Fig. 1H). This suggests that Nek2A's effect is only apparent in cells with supernumerary centrosomes that are already clustered. To test this hypothesis and assess the impact of Nek2A as a possible controller of centrosome clustering, we artificially increased the number of centrosomes through nocodazole treatment and PLK4 overexpression. Indeed, CA was successfully induced following these methods (Fig. 2A) in U2OS and MDA-MB-231 cells. Overexpressing PLK4 for 72 hours caused CA in about 40% of MDA-MB-231 and U2OS cell populations (Fig. 2B). Additionally, we induced CA in U2OS cells using the cytokinesis inhibitor DCB and STIL overexpression (Supplementary Fig. 2A, B). Post-amplification, metaphases were categorized as either bipolar clustered or multipolar. As observed in N1E-115 and SU86.86, Nek2A overexpression led to multipolar metaphases and significantly reduced centrosome clustering in MDA-MB-231 (Fig. 2C) and U2OS cells (Fig. 2D). In parallel with these results, overexpression of Nek2A induced significant increase in MPS formation in both of the alternative CA models, DCB and STIL overexpression respectively

(Supplementary Fig. 2C). The notable disruption of centrosome clustering by Nek2A overexpression during mitosis, without affecting the dispersion of supernumerary centrosomes in interphase (Fig. 1E, F), suggested that Nek2A's primary role was "prevention of clustering" rather than "unclustering" centrosomes. In order to distinguish between these processes, we performed live cell imaging and tracked the percentage of cells transitioning from bipolar to multipolar (unclustering) versus those starting as multipolar (prevention of clustering) (Supplementary Fig. 2D). Overexpression of both Nek2 and Plk4 resulted in decreased bipolar divisions, and bipolar cells at the metaphase plate never morphed into a multipolar shape ($n = 0$), indicating no unclustering. Multipolar cells could follow various fates, including adopting a bipolar shape (clustering), undergoing successful multipolar divisions, or failing division, leading to aneuploid cells or cell death (Supplementary Fig. 2E). Taken together, our data supports that Nek2A overexpression prevents centrosome clustering rather than un-clustering or de-clustering. Considering the natural bipolar division tendency of cellular forces, the default inclination by cellular machinery probably makes "preventing clustering" a more feasible approach than "unclustering" of the already coalesced centrosomes.

To investigate whether inference with Nek2A activity exerts the reverse effects, several approaches were undertaken including knockout, RNAi and using chemical inhibitor (JH295) targeting Nek2A in two different cell lines with CA induced with the aforementioned methods (Supplementary Fig. 2F). Consistent with our expectations, the results showed that suppression of Nek2A significantly decreased the percentage of MPS. To address whether the kinase activity of Nek2A is important for centrosome clustering, we overexpressed kinase-deficient mutant form of Nek2A (K37R substitution) [11], providing a dominant-negative (DN) phenotype. Over-expression of the DN mutant acted similarly to chemical and transcriptional inhibition of Nek2A, favouring centrosome clustering. Taken together, our data strongly argues that Nek2A regulates centrosome clustering which requires its kinase activity, in cancers cell with supernumerary centrosomes.

Nek2A overexpression promotes the depletion of cells with CA

Considering Nek2A overexpression's effect on centrosome clustering, we performed an in vitro competition assay to show its negative impact on cells with CA. We engineered U2OS and MDA-MB-231 cells for dox-inducible Nek2A and PLK4 overexpression (Supplementary Fig. 3A), labeling PLK4 and Nek2A co-expressors (Dox-Plk4&Nek2A) with H2B-mCherry and PLK4 expressors (Dox-Plk4) with H2B-eGFP (Fig. 3A). Co-culturing these cells with/without doxycycline for 10 days, we noted a marked decrease in mCherry-tagged cells, undergoing multipolar divisions from Nek2A overexpression, corroborated by flow cytometry and live-cell imaging (Fig. 3B, Supplementary Fig. 3B). We repeated this with MDA-MB-231 cells (Supplementary Fig. 3C) and SU86.86 cells using SU86.86(WT)-H2B-eGFP and SU86.86(dox-Nek2A)-H2B-mCherry (Supplementary Fig. 3D), observing similar effects. Control groups showed comparable proliferation rates. This indicates Nek2A overexpression's detrimental role in cells with supernumerary centrosomes, leading to cell death through multipolar divisions.

To ascertain whether the decrease in cell viability in these cells stemmed from programmed cell death pathways or a reduction in cell division, we assessed the population of cells positive for Annexin V (Fig. 3D) and examined Caspase 3/7 activity (Supplementary Fig. 3E) in cells that either overexpressed Nek2A without CA, exhibited CA without Nek2A overexpression, or had both conditions simultaneously. As we had predicted, only cells with both PLK4 and Nek2A overexpression underwent apoptosis, providing strong evidence that the prevention of centrosome clustering induced by Nek2A leads to the observed cell death phenotype only in the presence of supernumerary centrosomes.

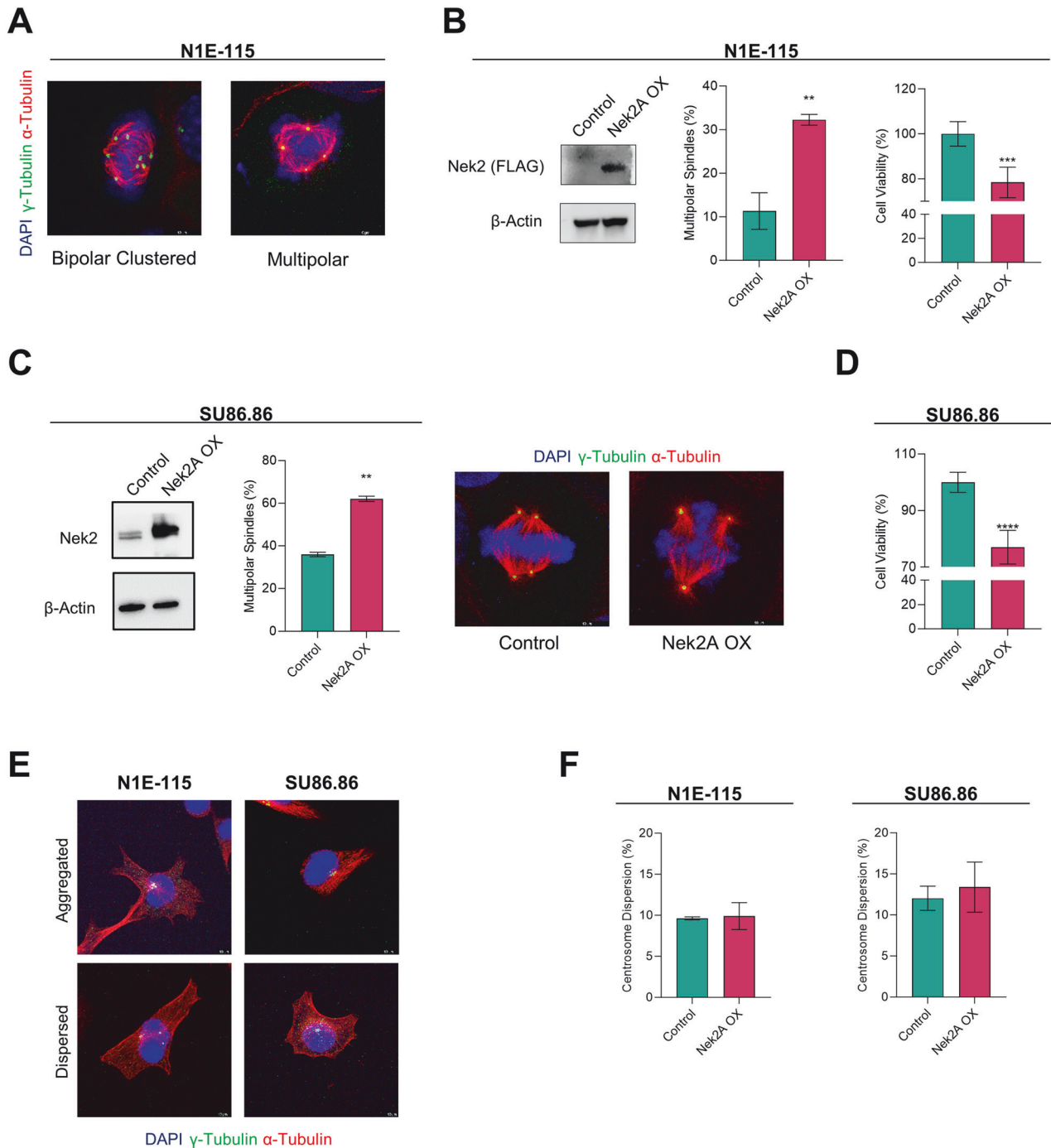


Fig. 1 Nek2 overexpression reduces centrosome clustering in cancer cells naturally comprising supernumerary centrosomes. **A** Representative IF staining images demonstrating supernumerary centrosomes, bipolar-clustered and multipolar metaphases observed in N1E-115 cells. **B** Ectopic overexpression of Nek2A confirmed by Western Blot (left), metaphase scoring indicating the induction of MPS formation (middle), and cell viability assay (right) in N1E-115 cells. **C** Overexpression of Nek2A confirmed by Western Blot (left), metaphase scoring (middle), and representative IF staining images (right) showing bipolar with clustered centrosomes and multipolar metaphases in SU86.86 cells. **D** WST-1 assay shows significant decrease in the viability of SU86.86 cells when Nek2A is overexpressed for 72 h. **E** Representative images demonstrating aggregated and dispersed localization of supernumerary centrosomes in N1E-115 and SU86.86 cells. **F** Percentage of centrosome dispersion in N1E-115 and SU86.86 cells. All experiments were performed as two biological repeats with at least 200 metaphases with CA scored per experiment. Error bars represent standard deviation from the mean. Statistical significance was shown as * $p < 0.05$, ** $p < 0.01$, *** $p < 0.001$, **** $p < 0.0001$. OX Overexpression.

Lastly, we conducted an in vivo version of the competition assay by subcutaneously implanting a mix of eGFP-tagged U2OS dox(PLK4) and mCherry-tagged U2OS Dox(PLK4&Nek2A) cells (Fig. 3E). After eight weeks, we analyzed the tumors and found a

significant reduction in Nek2A overexpressing (mCherry +) cells with CA (Fig. 3F). This demonstrates that Nek2A-induced multipolar divisions lead to cell depletion in both in vitro and in vivo settings.

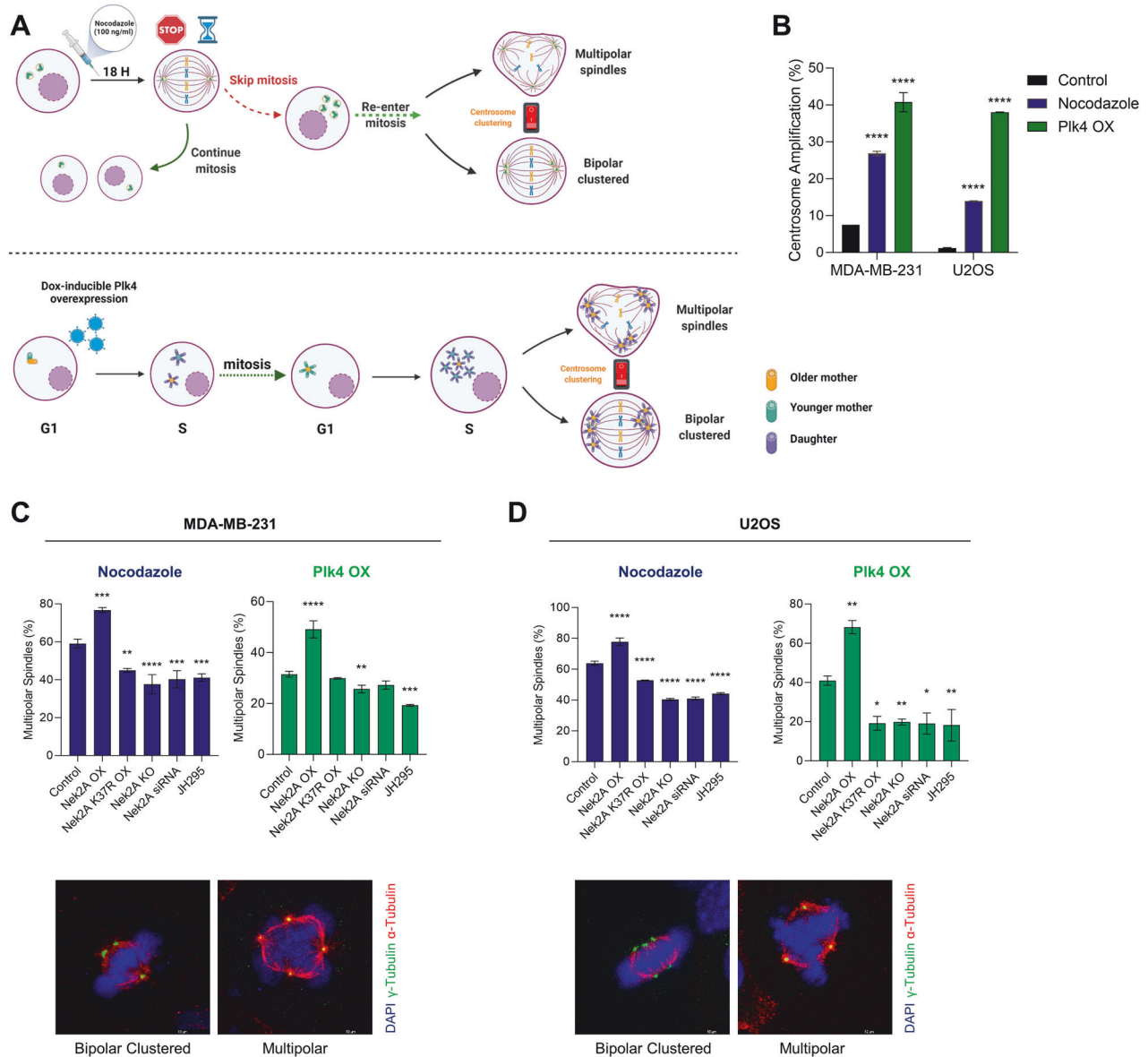


Fig. 2 **Nek2 regulates centrosome clustering in cells which are induced to have amplified centrosomes.** **A** Experimental setups to induce centrosome amplification by nocodazole (upper panel) and overexpression of PLK4 overexpression (lower panel). Created with BioRender. **B** Centrosome amplification levels obtained by nocodazole and PLK4 overexpression models. **C** Percentage multipolarity of MDA-MB-231 cells in nocodazole (top-left), PLK4 (top-right) models and representative images (bottom) showing bipolar clustered and multipolar metaphases. **D** Percentage multipolarity of U2OS cells in nocodazole (top-left), PLK4 (top-right) models and representative images (bottom) showing bipolar clustered and multipolar metaphases. Experiments were performed as two biological repeats with at least 200 metaphases with CA scored per experiment. Error bars show standard deviations. Statistical significance was shown as * $p < 0.05$, ** $p < 0.01$, *** $p < 0.001$, **** $p < 0.0001$. OX Overexpression, KO Knock-out.

Nek2A overexpression induces MPS independent of its intercentriolar linker and chromosomal targets

To comprehend the mechanism behind Nek2A's activity on centrosome clustering, we initially investigated the involvement of its possible targets. Nek2A kinase, known for regulating the centrosome cycle by phosphorylating C-Nap1 (CEP250) [7, 12], Rootletin (CROCC) [8, 13], and GAS2L1 [14, 15], also has non-centrosomal targets like Hec1 [16] and Trf1 [17] that may influence microtubule attachments and contribute prevention of centrosome clustering (Fig. 4A). We postulated that suppressing these targets would eliminate the observed phenotype resulting from Nek2A overexpression. Therefore, we generated monoclonal C-Nap1 and Rootletin knockout U2OS (dox-Nek2A) cells

(Supplementary Fig. 4A, B) and scored metaphases following induction of CA via two independent methods and Nek2A overexpression. As expected, Nek2A overexpression increased MPS and reduced bipolar clustered metaphases. Intriguingly, C-Nap1 knockout impaired centrosome clustering in both CA models, irrespective of Nek2A (Fig. 4B). In the nocodazole-induced CA model, Nek2A overexpression in C-Nap1 knockout cells resulted in a further decline in centrosome clustering, suggesting that absence of C-Nap1 promotes the formation of MPS independent of Nek2A activity. However, in the Plk4 CA model, Nek2A overexpression in C-Nap1 knockouts didn't further reduce clustered metaphases, indicating different CA mechanisms produce varied responses. These findings were

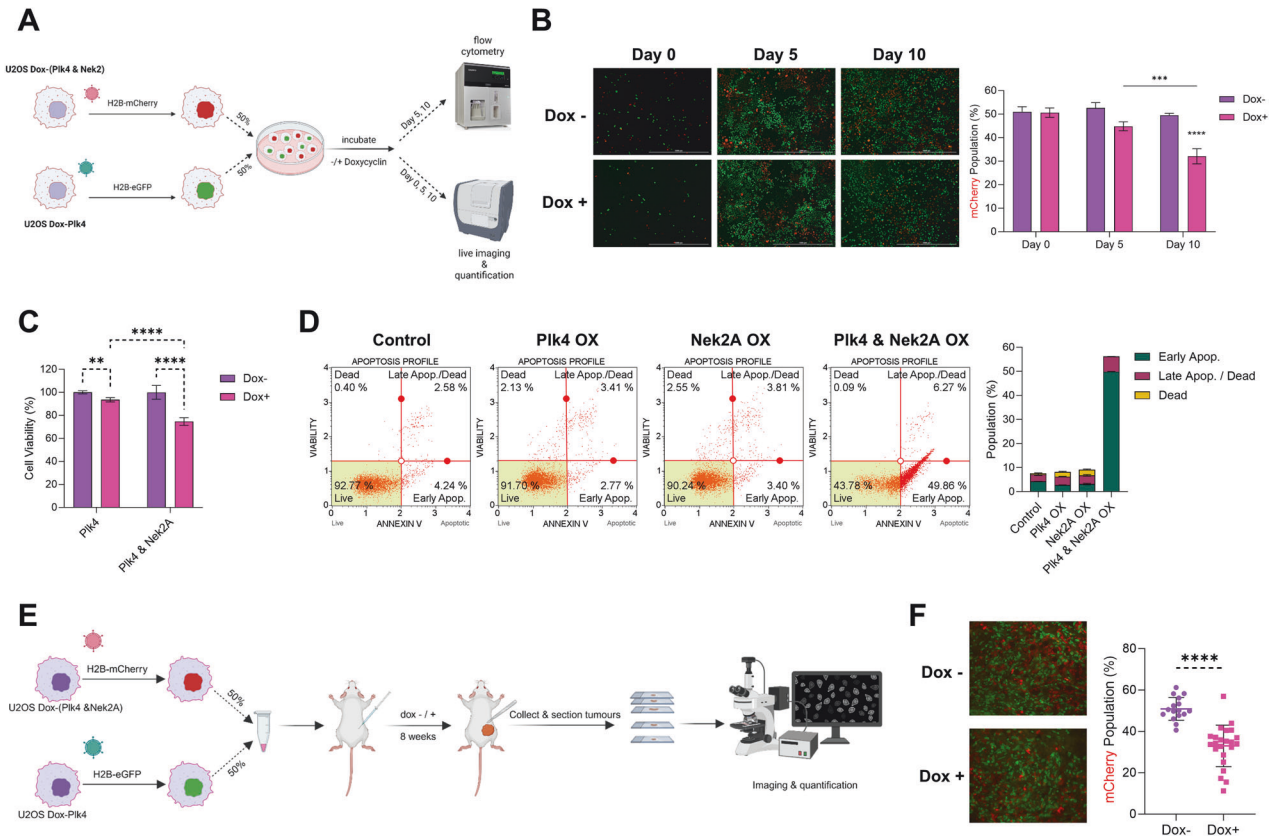


Fig. 3 Nek2A overexpression induces depletion of cells with centrosome amplification in vitro and in vivo. **A** Experimental setup of in vitro competition assay. Image created with BioRender. **B** Imaging-based analysis and quantification of mCherry-tagged U2OS cells co-overexpressing Plk4 and Nek2A. **C** WST-1 assay showing the significant decrease in cell viability as a result of Nek2A overexpression in cells with CA (induced by Plk4 overexpression). **D** Annexin V assay confirming the apoptosis induced by multipolar metaphases. **E** Experimental setup of in vivo competition assay. **F** Representative images of tumour tissue slices and quantification of mCherry-tagged U2OS Dox (PLK4 & Nek2) cells. Experiments were performed as at least 2 biological replicates. Error bars show standard deviations. Statistical significance was shown as * $p < 0.05$, ** $p < 0.01$, *** $p < 0.001$, **** $p < 0.0001$. OX Overexpression.

confirmed with independent monoclonal C-Nap1 knockout cells (Supplementary Fig. 4C).

To assess Rootletin's role in Nek2-induced prevention of centrosome clustering, we generated Rootletin knockout cells (Supplementary Fig. 4B) and examined metaphases post Nek2 overexpression in different CA models. Rootletin's absence reduced MPS formation in the Plk4 overexpression model but not in the nocodazole model, once again suggesting variances between the models (Fig. 4C). Additionally, Rootletin knockout slightly enhanced centrosome clustering in the Plk4 model, hinting at its independent role from Nek2A kinase. However, Rootletin's absence didn't negate Nek2A's effect (Fig. 4C).

We also analyzed C-Nap1 and Rootletin knockouts' impact on centrosome distance at interphase. As reported previously, immunofluorescence staining with anti- γ -tubulin antibodies showed C-Nap1 loss significantly increased the centrosome distance [18, 19], indicating potential dispersion-driven clustering disruption (Supplementary Fig. 4D). Nevertheless, Rootletin knockout didn't notably change centrosome distance.

Lastly, we investigated GAS2L1. Despite successful GAS2L1 suppression (Supplementary Fig. 4E), its loss didn't affect centrosome clustering or Nek2A-induced multipolarity any of the CA models (Fig. 4D).

Beyond Nek2A's centrosomal targets, we also investigated two non-centrosomal targets, TRF1 and Hec1, for their potential roles in centrosome clustering. Using siRNA to silence TRF1 (Supplementary Fig. 4F), we found that its suppression didn't affect

centrosome clustering in the nocodazole CA model nor did it prevent formation of MPS with Nek2A overexpression, even increasing multipolar metaphases in the Plk4 CA model (Fig. 4E). Further, Nek2A overexpression in TRF1-silenced cells still led to multipolar divisions, indicating TRF1's non-essential role in Nek2A-induced inhibition of centrosome clustering.

For Hec1, we treated U2OS cells with INH154, disrupting Nek2A-Hec1 interaction, and observed no significant impact on centrosome clustering or reversal of Nek2A overexpression effects during metaphase (Fig. 4F). Thus, our findings suggest that neither TRF1 nor Hec1 are key components in Nek2A's molecular mechanism.

Interaction between Nek2A and KIF2C mediates centrosome clustering

Since none of the known interactors of Nek2A appeared to be responsible for its effect on centrosome declustering, we hypothesized that a novel partner might be involved. Using the TurboID proximity labelling system and proteomic tools, we aimed to find unrecognized partners facilitating Nek2A to exert its effect on centrosome clustering in cancer (Fig. 5A). We first generated FLAG-TurboID-Nek2A and FLAG-TurboID-Nek2A(K37R) constructs (Supplementary Fig. 5A) and confirmed their cellular location (Fig. 5B), showing that both forms of Nek2A localizes to centrosomes similar to endogenous Nek2A. Additionally, streptavidin staining also confirmed that the majority of biotinylated proteins were centrosome-associated, suggesting that the identified and enriched proteins are

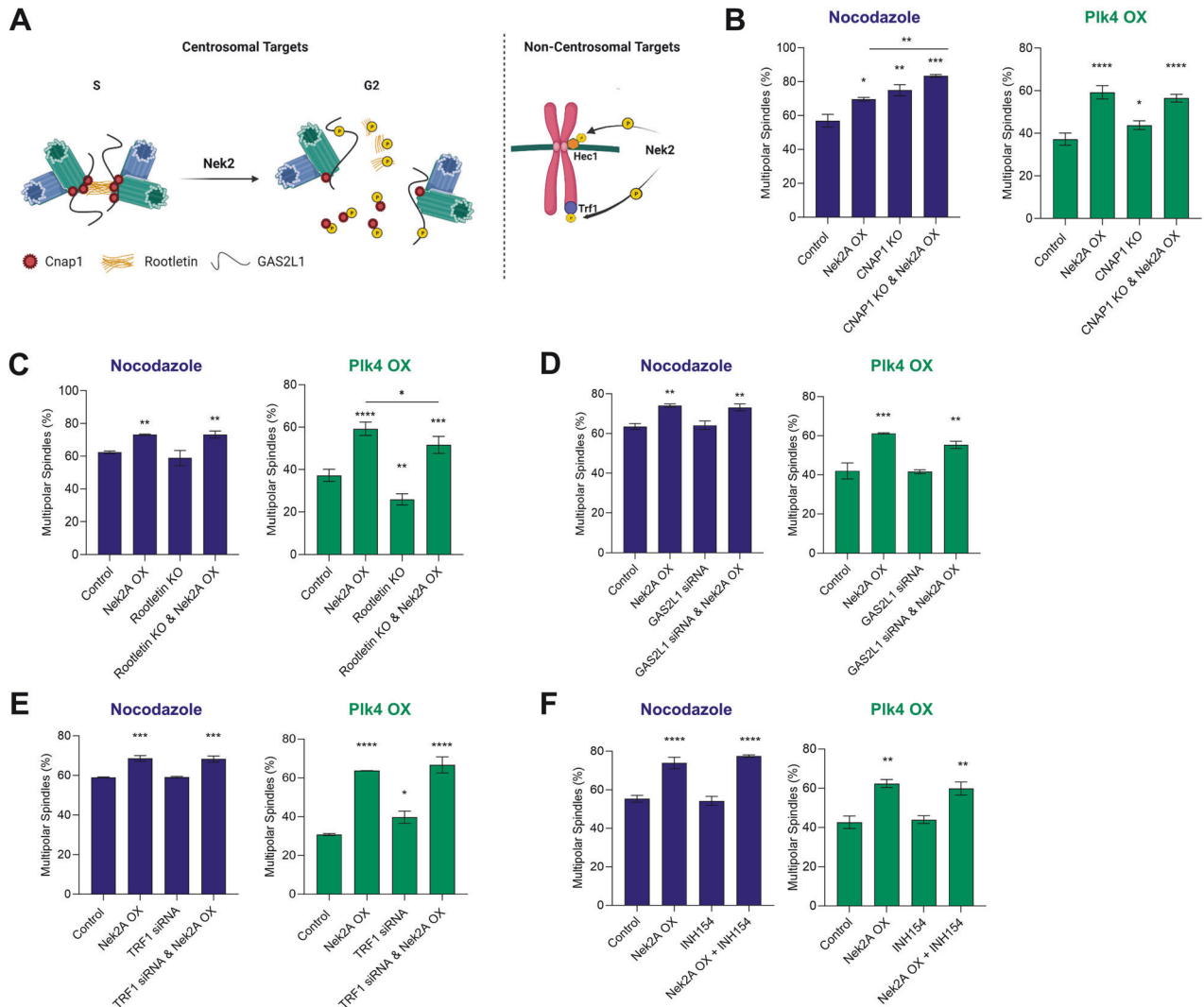


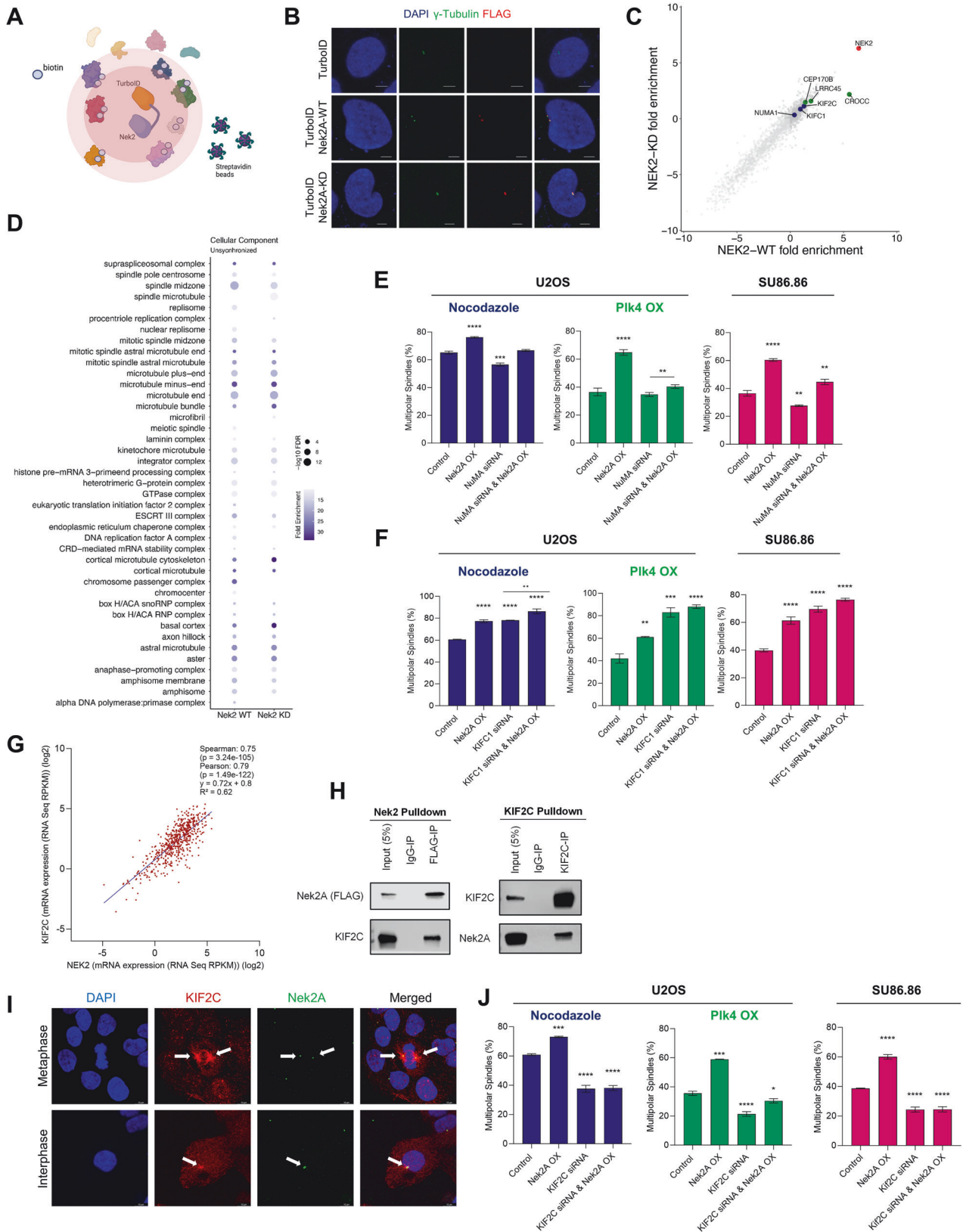
Fig. 4 Nek2A overexpression induces MPS formation independent of its intercentriolar linker and chromosomal targets. **A** Known centrosomal and non-centrosomal targets of Nek2A kinase. Image created by BioRender. Percentage MPS of U2OS cells in nocodazole and PLK4 models to examine effects of **B** C-Nap1, **C** Rootletin **D** GAS2L1, **E** TRF1, and **F** Hec1 (INH154 inhibits Nek2A-Hec1 interaction). Experiments were performed as two independent repeats with at least 200 metaphases with CA scored per experiment. Error bars show standard deviations. Statistical significance was shown as * $p < 0.05$, ** $p < 0.01$, *** $p < 0.001$, **** $p < 0.0001$. OX Overexpression, KO Knock-out.

probable participants in centrosome clustering mechanisms (Supplementary Fig. 5B). Our analysis confirmed known Nek2A interactors, validating our system's reliability. It identified biotinylated Nek2A targets (CROCC & LRRC45), known centrosome clustering regulators (NuMA & KIFC1), and potential new partners like KIF2C (Fig. 5C). The cellular component analysis revealed that both wild-type (WT) and kinase-deficient (KD) Nek2A primarily interact with proteins found in spindles and microtubules, demonstrating similar interaction profiles for both WT and KD forms. (Fig. 5D).

Finding KIFC1 and NuMA, known centrosome clustering factors, led us to explore their collaboration with Nek2A in this process. Depletion of NuMA is known to suppress the formation of MPS, while its overexpression disrupts centrosome clustering and increases the percentage of multipolarity [20]. We used siRNA to silence NuMA (Supplementary Fig. 5C) and consistent with prior reports [20], NuMA knockdown led to a marked reduction in the formation of MPS. Nevertheless, Nek2A overexpression was capable of inducing MPS without NuMA across three different experimental conditions, implying that Nek2A may govern a mechanism distinct from that of NuMA (Fig. 5E). Although NuMA silencing didn't impede Nek2A's overexpression

impact, there was a competitive interaction during the formation of MPS in metaphase, indicating they regulate centrosome clustering independently and antagonistically. Reversely, silencing Nek2A in NuMA-overexpressing cells also reduced centrosome clustering, further supporting their independent roles (Supplementary Fig. 5D, E). Next, we investigated how Nek2A interacts with KIFC1, another key centrosome clustering regulator. As reported earlier, silencing KIFC1 impaired centrosome clustering and increased multipolarity [21, 22]. Nek2A overexpression in KIFC1-silenced cells raised the percentage of multipolar metaphases, indicating that KIFC1 and Nek2A operate via distinct molecular pathways to orchestrate centrosome clustering (Fig. 5F). Supportingly, RNAi against Nek2A partially restored centrosome clustering in KIFC1-deficient cells (Supplementary Fig. 5F, G).

Analyzing proximity labeling data promoted us to study KIF2C's role, a kinesin family member. Intriguingly, analysis of cancer patient datasets revealed a strong correlation between the expressions of Nek2A and KIF2C (Spearman: 0.75, Pearson: 0.79, R^2 : 0.62) (Fig. 5G), suggesting a possible interaction between these proteins. Confirmatively, ectopically expressed FLAG-tagged



Nek2A in U2OS cells showed clear co-immunoprecipitation with KIF2C (Fig. 5H), and an anti-KIF2C antibody pull-down also captured Nek2A, verifying their physical interaction. Furthermore, immunofluorescent staining corroborated the colocalisation of

Nek2A and KIF2C at spindle poles (Fig. 5I). Overall, while the exact nature of this interaction remains unclear, it's evident that they associate closely and interact with each other, particularly in the vicinity of the centrosome.

Fig. 5 Proximity labelling and Co-IP reveals interaction between Nek2A and KIF2C regulating centrosome clustering. **A** Turbo-ID proximity labelling system to identify interaction partners of Nek2A. Image created with BioRender. **B** Cellular localization of TurboID-Nek2A verified by IF staining. **C** Plot showing enriched biotinylated proteins identified by Mass-Spec. Data was generated by MaxQuant LFQ analysis. Targets selected for further analysis were marked with blue colour, known interaction partners of Nek2A was colored green. **D** Cellular Component analysis on identified peptides in both WT and KD Nek2A interactome indicating sub-cellular localizations. **E, F** Percentage of multipolar metaphases observed in varying conditions for selected targets, NuMa and KIFC1. Experiments were performed using nocodazole and Plk4 CA models in U2OS and endogenously supernumerary centrosome harbouring cell line SU86.86. **G** Pan-cancer Analysis of Advanced and Metastatic Tumors data retrieved from cBioPortal demonstrates positive correlation between NEK2 and KIF2C expressions. **H** Co-IP assay to verify physical interaction between Nek2A and KIF2C. **I** IF staining demonstrating the co-localization of Nek2A and KIF2C in centrosomes and spindle poles. Arrowheads point to spindle poles and centrosomes where KIF2C and Nek2A co-localize. **J** Percentage of multipolar spindles observed when KIF2C is silenced. Experiments were performed as two biological repeats with at least 200 metaphases with CA scored per experiment. Error bars show standard deviations. Statistical significance was shown as * $p < 0.05$, ** $p < 0.01$, *** $p < 0.001$, **** $p < 0.0001$. KD Kinase-dead, WT Wild type, OX Overexpression.

As a novel Nek2A interactor, we assessed the impact of KIF2C knockdown in MPS formation in our CA models (Fig. 5J). KIF2C suppression significantly reduced multipolar metaphases in both models and cell lines. Notably, KIF2C depletion counteracted the effect of Nek2A overexpression, leading to reduced MPS formation. Our data suggests that the interaction between KIF2C and Nek2A is essential to regulate the clustering of supernumerary centrosomes during metaphase.

Further experiments were designed to determine if KIF2C ablation could impede the activity of Nek2A overexpression. We engineered U2OS cells with Nek2A overexpression, KIF2C shRNA expression and a combination of both in addition to Plk4 overexpression to induce CA (Supplementary Fig. 6A). In line with our earlier approach, competition experiments showed that suppressing KIF2C enhanced cell viability and proliferation, as evidenced by a marked reduction in multipolar metaphases (Fig. 6A and Supplementary Fig. 6B). Interestingly, overexpressing Nek2A did not result in multipolar metaphases, and consequently, cell death was avoided in cells treated with KIF2C shRNA. These observations were substantiated by cell viability assays (Fig. 6B) and Annexin-V staining (Fig. 6C and Supplementary Fig. 6C). Collectively, our data supports that KIF2C interaction is crucial for Nek2A's role in averting the clustering of supernumerary centrosomes, summarized and presented in (Fig. 6D).

To link our research to clinical applications, we investigated how high Nek2A levels and CA affect patient survival. Due to the lack of existing data on CA levels and gene expression in patient tumors, we initially analyzed the expression of five centrosomal genes (PLK4, CCNE1 (cyclin E), CETN2 (centrin-2), TUBG1 (γ -tubulin), and PCNT2 (pericentrin)), known as biomarkers for CA [23]. We modified and utilized a previously reported centrosome amplification index (CAI) as outlined in our methods section [23]. This involved using these genes' expression levels to determine the effect of elevated Nek2A expression on the survival of patients with high CAI. Our results revealed that patients with head and neck squamous cell carcinoma (HNSC), who had both high CAI and high Nek2A levels experienced notably better survival compared to those with high CAI but low Nek2A levels (Fig. 7A). Conversely, patients with low CAI experienced poorer outcomes when Nek2A levels were higher, aligning with its established phenotypes [24–27] (Fig. 7A, left panel). Next, we hypothesized that chemotherapy with microtubule inhibitors, similar to our nocodazole-induced amplification, might increase centrosome numbers. We then studied taxane response in patients with various Nek2A levels, finding those with higher levels responded better in several cancers (Fig. 7B and Supplementary Table 1). In these cohorts, we also analyzed the expression levels of CA biomarkers (PLK4, TUBG1, and CCNE1) and found higher expressions in patients who responded well to taxane treatment (Supplementary Fig. 7). Thus, although various elements affect the response to chemotherapy, the levels of Nek2A stand out as one of the predictors, likely as a result of its activity on centrosome clustering. Hence, although Nek2A seems like a promising target, its application must be carefully tailored based on the wider cellular environment, especially considering the level of centrosome amplification.

DISCUSSION

Overexpression of Nek2A in cancer cells is a double-edged sword. It is a facilitator of tumor growth, migration, and drug resistance, marking it as a prognostic indicator and a potential target in anticancer therapy [27–31]. However, high levels of aneuploidy can also induce cell death and hinder tumor progression. In our study, we explored the role of Nek2A in cells possessing supernumerary centrosomes. As normal cells typically have at most two centrosomes, they are expected to be less prone to deadly multipolar divisions when clustering mechanisms are prevented. Several studies support the notion that selectively targeting supernumerary centrosomes in cancer cells is a viable approach [21, 22, 32–34], and clustering inhibitors like CCCI-01 and GF15 can eliminate cancer cells while sparing normal cells, indicating a potential therapeutic window [35, 36]. We discovered that overexpression of Nek2A not only prevented clustering of these supernumerary centrosomes, but also decreased cell viability and increased apoptosis, likely due to the induction of multipolar divisions. MPS and subsequent cell death occurred selectively in cells with supernumerary centrosomes, while the viability of cells without centrosome amplification or without Nek2A overexpression remained unaffected. These findings suggest that the impact of Nek2A targeting can vary depending on the genetic and cellular context of the cancer cells, a consideration that has been largely neglected until now. Supporting this argument, Nek2A overexpression predicted better survival in HNSC patients with high centrosome amplification but worse outcomes in those with low amplification. Moreover, breast cancer patients with increased Nek2A expression had a more positive response to taxane treatment. We acknowledge that while this improvement could be due to centrosome amplification after taxane treatment, akin to our experimental results with nocodazole, other factors could also play a role.

Investigating Nek2A's role in centrosome clustering, we initially focused on potential centrosomal targets like C-Nap1, Rootletin, and Gas2L1. Consistent with literature, we found that the loss of C-Nap1 disrupts centrosome organization, increases centrosome distance, and leads to multipolar divisions [18, 19]. This effect is further amplified by KIFC1 inhibition in C-Nap1 knockout cells, indicating an independent role for C-Nap1 in centrosome clustering. Similarly, overexpressing Nek2A in these cells enhances multipolar metaphases, pointing to a synergistic effect with C-Nap1 in this process. Furthermore, Nek2A overexpression significantly increases multipolarity in cells lacking Rootletin, underscoring its influence beyond C-Nap1. Lastly, our findings suggest that GAS2L1, despite being a recent target of Nek2A [15], does not significantly impact centrosome clustering. This suggests that the effect of Nek2A overexpression is independent of the specific centrosomal targets during the G2/M transition.

Shifting focus to Nek2A's broader interactions, we explored its phosphorylation of mitotic proteins such as Hec1. Using INH154 to inhibit Nek2A-Hec1 interaction revealed that Hec1 is not essential for Nek2A-induced multipolar metaphases. Additionally, our study

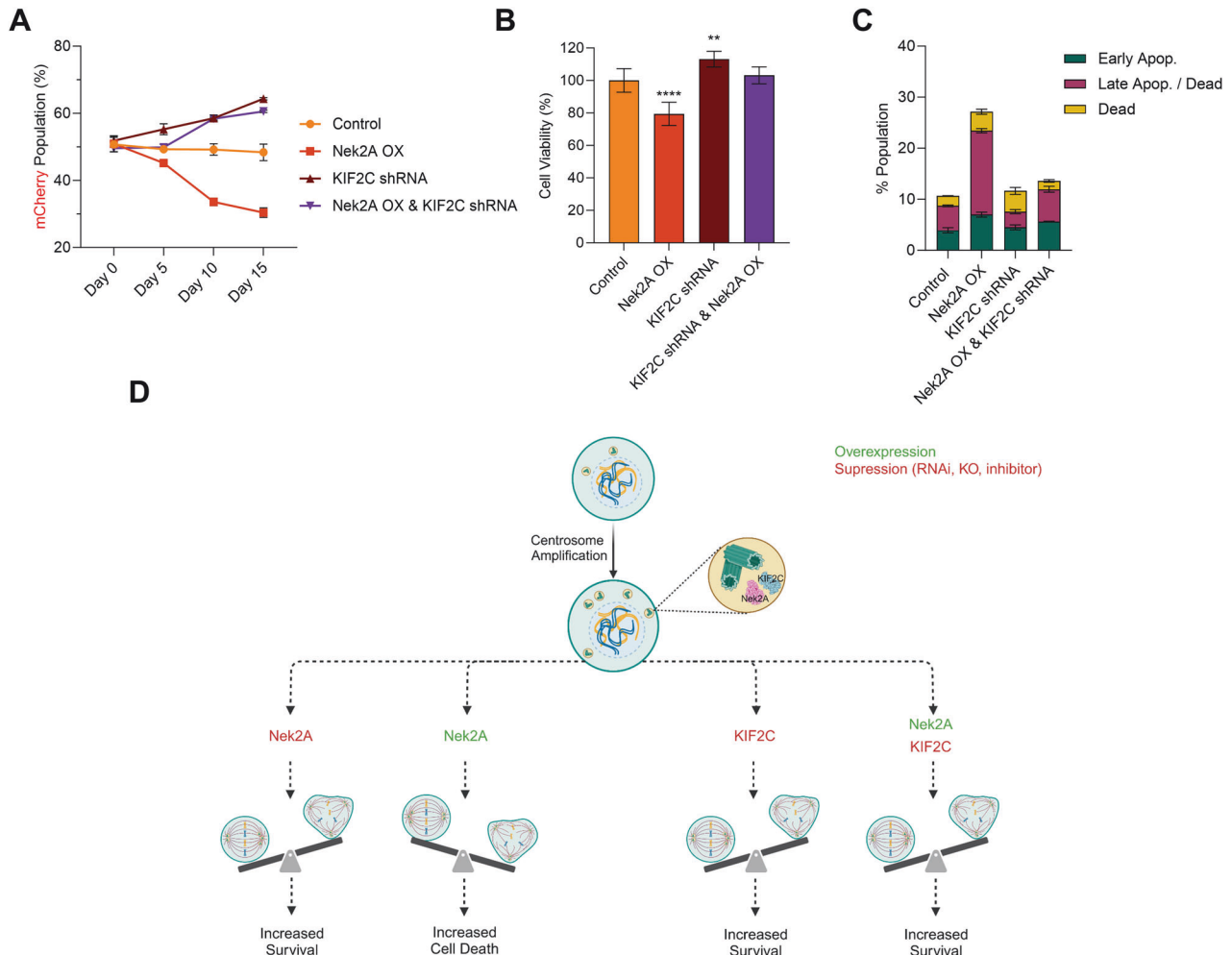


Fig. 6 KIF2C is required for Nek2A to prevent centrosome clustering. **A** Competition experiment result displays that suppression of KIF2C promotes cell survival in cells with supernumerary centrosomes. **B** WST-1 cell viability assay shows that suppression of KIF2C expression increases cell survival and attenuates the effect of Nek2A overexpression on survival of cells harbouring supernumerary centrosomes induced by Plk4 overexpression. **C** Annexin-V staining shows that suppression of KIF2C reverts apoptotic phenotype in Nek2A overexpressing cells harbouring Plk4-induced supernumerary centrosomes. **D** Schematic representation of the data demonstrating that Nek2A and KIF2C interaction in centrosomes and spindle poles regulate centrosome clustering and affect cancer cell survival. Image created with BioRender. Experiments were performed as two biological repeats. Error bars show standard deviations. Statistical significance was shown as * $p < 0.05$, ** $p < 0.01$, *** $p < 0.001$, **** $p < 0.0001$. OX Overexpression.

found that Nek2A's interaction with TRF1, though influential in cytokinesis in cells with centrosome amplification [17, 37], is not crucial for centrosome clustering. This comprehensive analysis leads us to propose that the effect of Nek2A overexpression involves novel targets, expanding the scope of Nek2A's impact in cellular processes. In our study, we utilized TurboID for efficient proximity labelling to explore Nek2A's interaction partners in centrosome clustering. The analysis identified 20 significantly enriched and previously known (BioGrid & IntAct databases) Nek2A interaction partners, including Nek2, with similar enrichment in both WT and KD pull-downs, suggesting that kinase function does not greatly change Nek2's interactome. Despite NuMA and KIF1 being identified within Nek2A-TurboID's labeling radius, our results show that Nek2A's ability to uncluster centrosomes is independent of these proteins. NuMA, which aids spindle bipolarization, is regulated by phosphorylation [38, 39] and plays a crucial role in tethering microtubules to the centrosomal region within the mitotic spindle. Depletion of NuMA hinders multipolar spindle pole formation, while its overexpression disrupts centrosome clustering, increasing the percentage of multipolar metaphases [20]. NuMA also contributes

to organizing k-fibers during human cell division by recognizing and clustering their loose ends at spindle poles, working in conjunction with motor proteins dynein and dynactin [40, 41].

Although clustering regulators NuMA and KIF1 were found within the labeling radius of Nek2A-TurboID, our results suggest that Nek2A's impact on centrosome clustering mechanisms operates independently of these proteins. NuMA is recognized for its role in tethering microtubules to the centrosomal region within the mitotic spindle, facilitating spindle bipolarization. The efficiency of this process is modulated by motor-generated forces that translocate NuMA to the centrosome and its cross-linking activity in that region. While NuMA clusters loose ends at the spindle poles, cooperating with the motor proteins dynein and dynactin [40, 41], it does not physically interact with Nek2A, as demonstrated by co-immunoprecipitation experiments. Despite NuMA's involvement in regulating centrosome clustering, our findings indicate that Nek2A operates independently of NuMA in this context.

Additionally, KIF1 was found to operate independently of Nek2A. Known for its role in centrosome clustering and tumorigenesis [22, 37, 38], KIF1 binds microtubules, promoting

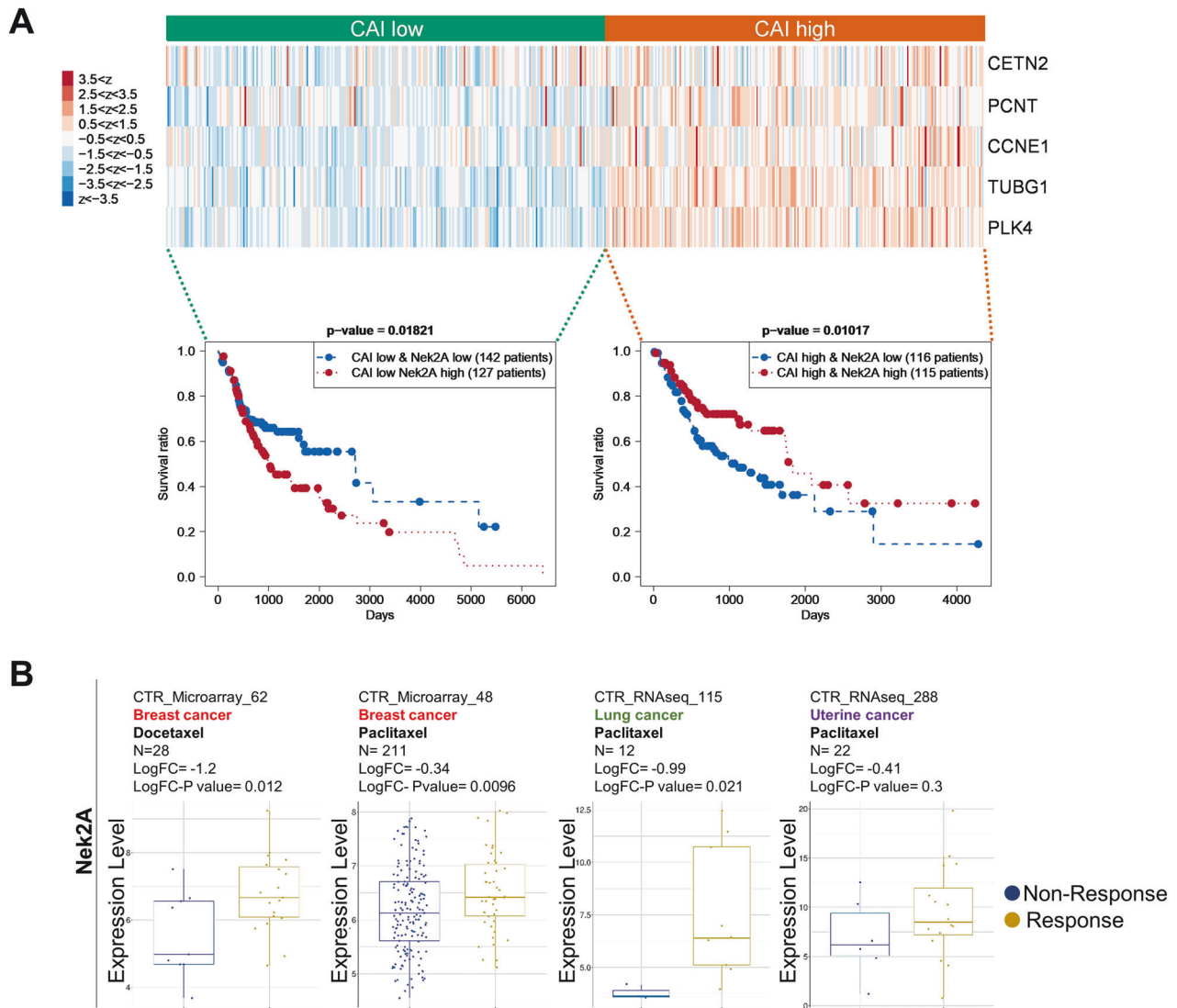


Fig. 7 Patient-derived clinical transcriptome data provides evidence that higher Nek2A expression improves survival and taxane response in patients with CA signatures. A TCGA data analysis indicates that high Nek2A expression significantly increases the survival rate of HNSC patients with high centrosome amplification index (CAI). **B** In cohorts of cancer patients exhibiting positive response to taxane treatment, relatively higher expression levels of Nek2A is observed compared to the non-responsive patients. Data was obtained from Cancer Treatment Response Gene Signature Data Base (CTR-DB).

their crosslinking near centrosomes [39]. It directly interacts with CEP215, facilitating the clustering of supernumerary centrosomes [40, 41]. KIF2C's significance in malignancy is highlighted by its identification as a dependency factor in breast cancers, with its phosphorylation triggered by DNA damage leading to centrosome clustering and drug resistance [42]. Inhibiting this phosphorylation reverses these effects, making KIF2C a potential therapeutic target. Our experiments show that Nek2A overexpression induces MPS even in the absence of KIF2C, and co-suppression partially restores centrosome clustering. This suggests independent control of centrosome clustering by Nek2A and KIF2C, acting as competitors in this process. This intricate balancing mechanism is supported by the positive correlation between their expressions [43], revealing that the overexpression of both proteins has contrasting effects on centrosome clustering.

KIF2C, a member of the kinesin-13 family known for regulating microtubule dynamics [42], has not been extensively studied in the context of centrosome clustering in human cancer. Recent findings indicate that both knockdown and overexpression of

KIF2C in HeLa cells increase multipolar metaphases, suggesting its activity is tightly regulated during mitosis [44]. Key regulatory mechanisms include phosphorylation by Aurora B, which inhibits KIF2C while guiding its centromere localization, and Aurora A [43, 45, 46]. Additionally, Cdk1 phosphorylation releases KIF2C from centrosomes and modulates its depolymerizing activity, while Plk1 phosphorylates both KIF2C and Nek2A, the latter promoting centrosome splitting [47–50].

Our study reveals a novel interaction between Nek2A and KIF2C in cancer cells with centrosome amplification, suggesting a coordinated regulation to maintain centrosome clustering. This interaction, validated through proximity labelling, co-staining, and co-immunoprecipitation, highlights the intricate relationship between mitotic kinases and kinesins in modulating microtubule dynamics and centrosome clustering during mitosis.

In this study, we have discovered a critical interaction between KIF2C and Nek2A that regulates centrosome clustering in cancer cells, marking the first identification of such a relationship. This interaction is most likely a kinase-substrate type, as evidenced by

our findings where overexpression of a kinase-dead Nek2A mutant acted dominantly negative, indicating the necessity of kinase activity for phenotypical outcomes. Further research is needed to elucidate the specifics of the KIF2C-Nek2A interaction.

CONCLUSION

In conclusion, this study illuminates the crucial role of Nek2A in controlling centrosome clustering in cancer cells, particularly those with supernumerary centrosomes. Overexpression of Nek2A represents a disadvantage for cancer cells with supernumerary centrosomes, shown under both *in vitro* and *in vivo* conditions. Silencing KIF2C rescues the cells from the detrimental effect of Nek2A. This study highlights the potential of targeting Nek2A and its interactors, like KIF2C, for novel cancer therapies aimed at managing centrosome-related genomic instability. Further exploration of these molecular interactions promises to enhance our understanding of centrosome clustering regulation and its significance in cancer biology, opening new avenues for effective cancer treatment strategies.

MATERIAL AND METHODS

Cell culture

N1E115 (ATCC, CRL-2263), MDA-MB-231 (ATCC, HTB-26), U2OS (ATCC, HTB-96), SU86.86 (ATCC, CRL-1837), MIA PaCa-2 (ATCC, CRL-1420), Panc1 (ATCC, CRL-1469), HEK293T (ATCC, CRL-3216) were maintained in DMEM (Gibco) supplemented with 10% FBS (Gibco) and 1% Pen/Strep (Gibco) at 37 °C and 5% CO₂ incubator.

Plasmids

Nek2A (clone ID: 38963) in pJP1563 and NuMA1 (clone ID: 871325) in pLenti6.3/V5-DEST were purchased from DNASU. LentiCRISPR-v2 (52961), pCW57-RFP-P2A-MCS (78933), pCW57-MCS1-P2A-MCS2 (80922), pCDH-EF1-FHC (64874), Flag-TurboID (124646), Tet-pLKO-neo (21916), pCDNA3-Plk4 (41165), pCDNA5-STIL (80266), PGK-H2B-mCherry (21217) and PGK-H2B-eGFP (21210) were purchased from Addgene.

Kinase-dead mutant (K37R) of Nek2A was derived from Nek2A in pJP1563 using Q5 Site-Directed Mutagenesis Kit (NEB) following the instructions of manufacturer. Oligos used for the SDM reaction are given in (Supplementary Table 2). Single guide RNA (sgRNA) oligos (Supplementary Table 3) for CRISPR/Cas9 knockout of Nek2A, C-Nap1 and Rootletin were cloned into LentiCRISPR-v2 as previously described [51]. Dox-inducible overexpressions of Nek2A and PLK4 were achieved by subcloning to pCW57-RFP-P2A-MCS and pCW57-MCS1-P2A-MCS2 respectively. Nek2A-WT and Nek2A-KD(K37R) cDNAs were subcloned to Flag-TurboID. To perform Co-IP using anti-FLAG antibody, Nek2A cDNA was subcloned into pCDH-EF1-FHC. Oligos for dox-inducible shRNA expression targeting KIF2C were cloned into Tet-pLKO-neo as previously described [52] and provided in (Supplementary Table 4).

Transfection and viral transduction

Nek2A, Gas2L1, TRF1, NuMA, KIFC1 and KIF2C were silenced by siRNA transfections. A list of the siRNAs is provided in (Supplementary Table 5). Briefly, 2×10^5 cells were seeded in 6 well plates, 100 pmol siRNA, and 7.5 μ l of Lipofectamine 3000 (Thermo) were added to culture media according to the manufacturer's protocol. Knock-down efficiencies were analysed by either Western Blot or RT-qPCR or both.

Overexpressions (Nek2A, PLK4, NuMA), CRISPR/Cas9-mediated knockouts and shRNAs were delivered to target cells via viral particles. To generate viral particles, 2×10^6 HEK293T cells were seeded per 10 cm petri dish. 2500 ng transfer vector, 2250 ng packaging vector (psPAX2 for lentivirus, pJMVC for retrovirus) and 250 ng envelope vector (pCMV-VSV-G) are mixed with 20 μ l Fugene 6 (Roche, USA) diluted in OptiMEM. Cells were transfected with the mixture prepared. Culture medium was collected 48- and 72-hours post-transfection and 100 \times concentrated by 50% (w/v) PEG 8000 (P2139, Sigma). Infections were performed using 10 μ l virus and 8 μ g/ml protamine sulphate in 2 ml culture medium.

Centrosome amplification using microtubule inhibitor

2×10^5 cells were seeded on 15×15 mm coverslips. Nocodazole (100 ng/ml) treatment was done for 16 hours to achieve prometaphase arrest and mitotic slip, resulting in duplicated centrosomes. Culture media was

replenished without nocodazole, and cells were incubated 24 h to allow cells to recover and re-enter the cell cycle with amplified centrosomes.

Immunofluorescence staining

Cells grown on coverslips were fixed with ice-cold methanol for 15 minutes, washed 3 times with DPBS-T, and blocked with 5% (w/v) BSA for 30 minutes. Samples were incubated with primary antibodies for γ -Tubulin (SIGMA, T5192), α -Tubulin (Abcam, 7291), Nek2 (BD Biosciences, 610593), FLAG (SIGMA, F1804), KIF2C (Santa Cruz, sc-81305) (1:500 dilution in 1% BSA in PBS) at 4 °C overnight, followed by incubation at RT for 2 hours with secondary antibodies (1:1000 dilution in 1% BSA in PBS) (Alexa flour 488 and 594, Thermo). Cell nuclei were labelled by DAPI containing mounting medium (Vectashield).

RT-qPCR

Total RNA is isolated using NucleoSpin RNAII kit (Macherey-Nagel) following the manufacturer's instructions. 1000 ng total RNA is reverse transcribed using M-MLV Reverse Transcriptase (Invitrogen) cDNA synthesis kit following the manufacturer's protocol. RT-qPCR is performed using The LightCycler 480 SYBR Green I (Roche), and the reaction was run at LightCycler 480 Instrument II (Roche). Samples were normalised to GAPDH expression. The PCR products are subjected to a melting curve analysis. Primers used in this study are provided in (Supplementary Table 6).

Western Blot

Cell pellets were lysed in RIPA buffer (50 mM Tris, pH 7.4, 500 mM NaCl, 0.4% SDS, 5 mM EDTA, 1 mM DTT, 2% Triton X-100, with protease and phosphatase inhibitors). Samples are run on SDS-PAGE for separation and then transferred to PVDF membranes. Membranes are blocked with 5% non-fat dry milk in 1X TBS-T and then incubated overnight at 4 °C with primary antibodies with recommended or optimised dilutions. Membranes were washed 3 times with TBS-T and incubated with corresponding secondary antibodies at RT for 2 hours. Blots are visualised using the Licor Odyssey FC imaging system. Beta-actin was used as the loading control.

Metaphase scoring

Cells were stained for γ -Tubulin and DAPI and a minimum of 300 metaphases with CA/experiment were scored and each experiment was repeated at least twice. CA was measured based on centrosome number per cell at interphase. Cells bearing >2 centrosomes were marked as CA.

Cell viability

Cell viability was determined with WST-1 assay: 3000 cells/well were seeded in 96-well plates, adhered overnight (16 h), followed by a 30-min incubation with WST-1 reagent (Roche) and absorbance read at 440 nm using a microplate reader (Synergy H1 Reader, Biotek, USA).

Cell cycle and apoptosis assays

Cell cycle analysis was performed using the Muse Cell Cycle Assay Kit (Millipore). The Annexin V staining procedure was conducted using the Muse[®] Annexin V & Dead Cell Kit from Luminex (MCH100105), following the provided manufacturer's guidelines. Flow cytometry analysis was conducted using the Muse Cell Analyzer, and the data were processed using Muse analysis software.

Dual-color competition assays

The long-term effects on cell survival and proliferation were assessed using dual-color competition assays *in vitro* and *in vivo*. Cells were tagged with either mCherry or eGFP and mixed in a 1:1 ratio. For *in vitro* assays, 5×10^4 cells were seeded in 6-well plates and passaged 1:5 at confluence. Plates were imaged at day 0, 5, 10, and 15 using an Agilent BioTek Cytation 5 imaging platform. mCherry-positive cells were quantified using Cytation 5 software. For *in vivo* assays, 100 μ l of a 1:1 mixture of 2×10^7 cells/ml in Matrigel was injected subcutaneously into 8–10 weeks-old, male, SCID mice. After 8 weeks, 6 tumors were collected, fixed, dehydrated, cleared, and paraffin-embedded. 2 μ m sections were obtained using microtome (Leica RM2245) picked randomly to represent different parts of the tumor.

TurboID proximity labelling

Cell pellets were obtained by centrifugation following biotinylation and PBS washes. Protein lysates were prepared by incubating cell pellets with protease inhibitor in lysis buffer. Protein concentrations were determined using the BCA method, and proteins were subjected to overnight incubation with Streptavidin beads at 4 °C. Beads were washed twice to remove unbound proteins, and bound proteins were subsequently subjected to trypsin digestion. Following digestion, formic acid was added to the samples to achieve a final concentration of 5%. The resulting supernatants were collected and analyzed using a Thermo Scientific Q Exactive HF Hybrid Quadrupole-Orbitrap Mass Spectrometer. Peptide identification and quantification were performed using Thermo Fisher Scientific Proteome Discoverer and MaxQuant software. Known contaminant proteins, such as keratin, were excluded from the analysis, and proteins identified with at least two unique peptides were considered significant in terms of abundance.

Co-Immunoprecipitation (Co-IP)

Cells were harvested via trypsinization, crosslinked with 0.1% paraformaldehyde (PFA) for 7 min, and lysed directly in ice-cold immunoprecipitation (IP) buffer supplemented with protease inhibitor, phosphatase inhibitor, and PMSF. Protein concentration was determined using a BCA assay. Protein G magnetic beads were pre-cleared and incubated with protein samples and specific antibodies or IgG control for 2 h at 4 °C. Following overnight incubation with protein G magnetic beads, beads were washed three times with IP buffer, and proteins were eluted by denaturation with 1× Laemmli buffer containing 50 mM DTT at 95 °C for 15 min. Western blotting was employed for subsequent analysis.

Microscopy

Leica DMI8 SP8 microscope and LASX software was used for confocal imaging, live-cell imaging and image processing. For live-cell imaging, PLK4 overexpressing U2OS-H2B-mCherry cells were synchronized by double-thymidine treatment [53], metaphase cells were tracked and recorded based on the fate of division. Metaphase scoring was performed using Carl Zeiss Axio Imager M1. Competition assays were performed by using BioTek Cytation 5 Cell Imaging Multimode Reader.

Patient data analysis

Gene expression data for tumors were processed using The Cancer Genome Atlas (TCGA) consortium's RNA-Seq pipeline (<https://portal.gdc.cancer.gov>). We downloaded HTSeq-FPKM files for all primary tumors from the latest data release (Data Release 38–August 31, 2023), excluding metastatic tumors due to their distinct biology. Patient survival data were extracted from clinical annotation files. Our survival analysis included only patients with both survival data and gene expression profiles. We \log_2 -transformed and z-normalized the gene expression profiles within each cohort, generating heat maps from these normalized values. For gene set analyses, we used *k*-means clustering (*k* = 2) on the normalized data, comparing Kaplan-Meier survival curves for the two groups via a log-rank test. We further divided each group based on Nek2A expression to examine its impact on survival.

CTR-DB (Cancer Treatment Response gene signature DataBase) [54] was used to process patient transcriptome data along with taxane response and expression levels of Nek2A, KIF2C, and centrosome amplification biomarkers PLK4, TUBG1, and CCNE1.

Statistical analysis

All experiments were conducted as biological repeats, and statistical analysis was performed using GraphPad Prism version 9.0. The student's *t*-test was employed to compare two groups, while the two-way ANOVA was used to compare more than two groups for parametric variables. Significance levels were denoted as follows: * for $p < 0.05$, ** for $p < 0.01$, and *** for $p < 0.001$.

DATA AVAILABILITY

The mass spectrometry proteomics data have been deposited to the ProteomeXchange Consortium via the PRIDE [55] partner repository with the dataset identifier PXD046867.

REFERENCES

- Song S, Jung S, Kwon M. Expanding roles of centrosome abnormalities in cancers. *BMB Rep.* 2023;56:216–24.
- Kalkan BM, Ozcan SC, Quintyne NJ, Reed SL, Acilan C. Keep calm and carry on with extra centrosomes. *Cancers.* 2022;14:442.
- Godinho SA, Pellman D. Causes and consequences of centrosome abnormalities in cancer. *Philos Trans R Soc Lond B Biol Sci.* 2014;369:20130467.
- Fry AM, Meraldi P, Nigg EA. A centrosomal function for the human Nek2 protein kinase, a member of the NIMA family of cell cycle regulators. *EMBO J.* 1998;17:470–81.
- Fry AM. The Nek2 protein kinase: a novel regulator of centrosome structure. *Oncogene.* 2002;21:6184–94.
- O'ryan L, Blot J, Fry AM. Mitotic regulation by NIMA-related kinases. *Cell Div.* 2007;2:1–12.
- Fry AM, Mayor T, Meraldi P, Stierhof Y-D, Tanaka K, Nigg EA. C-Nap1, a novel centrosomal coiled-coil protein and candidate substrate of the cell cycle-regulated protein kinase Nek2. *J Cell Biol.* 1998;141:1563–74.
- Bahe S, Stierhof Y-D, Wilkinson CJ, Leiss F, Nigg EA. Rootletin forms centriole-associated filaments and functions in centrosome cohesion. *J Cell Biol.* 2005;171:27–33.
- Ring D, Hubble R, Kirschner M. Mitosis in a cell with multiple centrioles. *J Cell Biol.* 1982;94:549–56.
- Mittal K, Ogden A, Reid MD, Rida PCG, Varambally S, Aneja R. Amplified centrosomes may underlie aggressive disease course in pancreatic ductal adenocarcinoma. *Cell Cycle.* 2015;14:2798–809.
- Faragher AJ, Fry AM. Nek2A kinase stimulates centrosome disjunction and is required for formation of bipolar mitotic spindles. *Mol Biol Cell.* 2003;14:2876–89.
- Mayor T, Hacker U, Stierhof YD, Nigg EA. The mechanism regulating the dissociation of the centrosomal protein C-Nap1 from mitotic spindle poles. *J Cell Sci.* 2002;115:3275–84.
- Yang J, Adamian M, Li T. Rootletin interacts with C-Nap1 and may function as a physical linker between the pair of centrioles/basal bodies in cells. *Mol Biol Cell.* 2006;17:1033–40.
- Au FK, Jia Y, Jiang K, Grigoriev I, Hau BK, Shen Y, et al. GAS2L1 is a centriole-associated protein required for centrosome dynamics and disjunction. *Dev Cell.* 2017;40:81–94.
- Au FK, Hau BKT, Qi RZ. Nek2-mediated GAS2L1 phosphorylation and centrosome-linker disassembly induce centrosome disjunction. *J Cell Biol.* 2020;219:e201909094.
- Chen Y, Riley DJ, Zheng L, Chen P-L, Lee W-H. Phosphorylation of the mitotic regulator protein Hec1 by Nek2 kinase is essential for faithful chromosome segregation. *J Biol Chem.* 2002;277:49408–16.
- Prime G, Markie D. The telomere repeat binding protein Trf1 interacts with the spindle checkpoint protein Mad1 and Nek2 mitotic kinase. *Cell Cycle.* 2005;4:121–4.
- Panic M, Hata S, Neuner A, Schiebel E. The centrosomal linker and microtubules provide dual levels of spatial coordination of centrosomes. *PLoS Genet.* 2015;11:e1005243.
- Theile L, Li X, Dang H, Mersch D, Anders S, Schiebel E. Centrosome linker diversity and its function in centrosome clustering and mitotic spindle formation. *EMBO J.* 2023;42:e109738.
- Quintyne NJ, Reing JE, Hoffelder DR, Gollin SM, Saunders WS. Spindle multipolarity is prevented by centrosomal clustering. *Science.* 2005;307:127–9.
- Leber B, Maier B, Fuchs F, Chi J, Riffel P, Anderhub S, et al. Proteins required for centrosome clustering in cancer cells. *Sci Transl Med.* 2010;2:33ra8–ra8.
- Kwon M, Godinho SA, Chandhok NS, Ganem NJ, Azioune A, Thery M, et al. Mechanisms to suppress multipolar divisions in cancer cells with extra centrosomes. *Genes Dev.* 2008;22:2189–203.
- Pannu V, Mittal K, Cantuarua G, Reid MD, Li X, Donthamsetty S, et al. Rampant centrosome amplification underlies more aggressive disease course of triple negative breast cancers. *Oncotarget.* 2015;6:10487.
- Xu H, Zeng L, Guan Y, Feng X, Zhu Y, Lu Y, et al. High NEK2 confers to poor prognosis and contributes to cisplatin-based chemotherapy resistance in nasopharyngeal carcinoma. *J Cell Biochem.* 2019;120:3547–58.
- Wang C, Huang Y, Ma X, Wang B, Zhang X. Overexpression of NEK2 is correlated with poor prognosis in human clear cell renal cell carcinoma. *Int J Immunopathol Pharm.* 2021;35:20587384211065893.
- Zeng Y-R, Han Z-D, Wang C, Cai C, Huang Y-Q, Luo H-W, et al. Overexpression of NIMA-related kinase 2 is associated with progression and poor prognosis of prostate cancer. *BMC Urol.* 2015;15:1–8.
- Kokuryo T, Yokoyama Y, Yamaguchi J, Tsunoda N, Ebata T, Nagino M. NEK2 is an effective target for cancer therapy with potential to induce regression of multiple human malignancies. *Anticancer Res.* 2019;39:2251–8.
- Li Y, Chen L, Feng L, Zhu M, Shen Q, Fang Y, et al. NEK2 promotes proliferation, migration and tumor growth of gastric cancer cells via regulating KDM5B/H3K4me3. *Am J Cancer Res.* 2019;9:2364–78.

29. Bai R, Yuan C, Sun W, Zhang J, Luo Y, Gao Y, et al. NEK2 plays an active role in tumorigenesis and tumor microenvironment in non-small cell lung cancer. *Int J Biol Sci.* 2021;17:1995–2008.
30. Zhou W, Yang Y, Xia J, Wang H, Salama ME, Xiong W, et al. NEK2 induces drug resistance mainly through activation of efflux drug pumps and is associated with poor prognosis in myeloma and other cancers. *Cancer Cell.* 2013;23:48–62.
31. Cusan M, Wang L. NEK2, a promising target in TP53 mutant cancer. *Blood Sci.* 2022;04:97–8.
32. Rebacz B, Larsen TO, Clausen MH, Rønneest MH, Löffler H, Ho AD, et al. Identification of griseofulvin as an inhibitor of centrosomal clustering in a phenotype-based screen. *Cancer Res.* 2007;67:6342–50.
33. Choe MH, Kim J, Ahn J, Hwang SG, Oh JS, Kim JS. Centrosome clustering is a tumor-selective target for the improvement of radiotherapy in breast cancer cells. *Anticancer Res.* 2018;38:3393.
34. Navarro-Serer B, Childers EP, Hermance NM, Mercadante D, Manning AL. Aurora A inhibition limits centrosome clustering and promotes mitotic catastrophe in cells with supernumerary centrosomes. *Oncotarget.* 2019;10:1649–59.
35. Kawamura E, Fielding AB, Kannan N, Balgi A, Eaves CJ, Roberge M, et al. Identification of novel small molecule inhibitors of centrosome clustering in cancer cells. *Oncotarget.* 2013;4:1763–76.
36. Raab MS, Breitzkreutz I, Anderhub S, Rønneest MH, Leber B, Larsen TO, et al. GF-15, a novel inhibitor of centrosomal clustering, suppresses tumor cell growth in vitro and in vivo. *Cancer Res.* 2012;72:5374–85.
37. Ohishi T, Muramatsu Y, Yoshida H, Seimiya H. TRF1 ensures the centromeric function of Aurora-B and proper chromosome segregation. *Mol Cell Biol.* 2014;34:2464–78.
38. Chinen T, Yamamoto S, Takeda Y, Watanabe K, Kuroki K, Hashimoto K, et al. NuMA assemblies organize microtubule asters to establish spindle bipolarity in acentrosomal human cells. *EMBO J.* 2020;39:e102378.
39. Zeng C. NuMA: a nuclear protein involved in mitotic centrosome function. *Microsc Res Tech.* 2000;49:467–77.
40. Hueschen CL, Kenny SJ, Xu K, Dumont S. NuMA recruits dynein activity to microtubule minus-ends at mitosis. *Elife.* 2017;6:e29328.
41. van Toorn M, Gooch A, Boerner S, Kiyomitsu T. NuMA deficiency causes micronuclei via checkpoint-insensitive k-fiber minus-end detachment from mitotic spindle poles. *Curr Biol.* 2023;33:572–80.
42. Ritter A, Kreis N-N, Louwen F, Wordeman L, Yuan J. Molecular insight into the regulation and function of MCAK. *Crit Rev Biochem Mol Biol.* 2016;51:228–45.
43. Zhang X, Ems-McClung SC, Walczak CE. Aurora A phosphorylates MCAK to control ran-dependent spindle bipolarity. *Mol Biol Cell.* 2008;19:2752–65.
44. Moon HH, Kreis NN, Friemel A, Roth S, Schulte D, Solbach C, et al. Mitotic Centromere-Associated Kinesin (MCAK/KIF2C) regulates cell migration and invasion by modulating microtubule dynamics and focal adhesion turnover. *Cancers (Basel).* 2021;13:5673.
45. Andrews PD, Ovechkinina Y, Morrice N, Wagenbach M, Duncan K, Wordeman L, et al. Aurora B regulates MCAK at the mitotic centromere. *Dev Cell.* 2004;6:253–68.
46. Lan W, Zhang X, Kline-Smith SL, Rosasco SE, Barrett-Wilt GA, Shabanowitz J, et al. Aurora B phosphorylates centromeric MCAK and regulates its localization and microtubule depolymerization activity. *Curr Biol.* 2004;14:273–86.
47. Sanhaji M, Friel CT, Kreis N-N, Krämer A, Martin C, Howard J, et al. Functional and spatial regulation of mitotic centromere-associated kinesin by cyclin-dependent kinase 1. *Mol Cell Biol.* 2010;30:2594–607.
48. Zhang W, Fletcher L, Muschel RJ. The role of Polo-like kinase 1 in the inhibition of centrosome separation after ionizing radiation. *J Biol Chem.* 2005;280:42994–9.
49. Zhang L, Shao H, Huang Y, Yan F, Chu Y, Hou H, et al. PLK1 phosphorylates MCAK and promotes its depolymerase activity. *J Biol Chem.* 2010.
50. Mbom BC, Siemers KA, Ostrowski MA, Nelson WJ, Barth AI. Nek2 phosphorylates and stabilizes β -catenin at mitotic centrosomes downstream of Plk1. *Mol Biol Cell.* 2014;25:977–91.
51. Sanjana NE, Shalem O, Zhang F. Improved vectors and genome-wide libraries for CRISPR screening. *Nat Methods.* 2014;11:783–4.
52. Wiederschain D, Wee S, Chen L, Loo A, Yang G, Huang A, et al. Single-vector inducible lentiviral RNAi system for oncology target validation. *Cell Cycle.* 2009;8:498–504.
53. Ozcan SC, Kalkan BM, Cicek E, Canbaz AA, Acilan C. Prolonged overexpression of PLK4 leads to formation of centriole rosette clusters that are connected via canonical centrosome linker proteins. *Sci Rep.* 2024;14:4370.
54. Liu Z, Liu J, Liu X, Wang X, Xie Q, Zhang X, et al. CTR-DB, an omnibus for patient-derived gene expression signatures correlated with cancer drug response. *Nucleic Acids Res.* 2022;50:D1184–d99.
55. Perez-Riverol Y, Bai J, Bandla C, García-Seisdedos D, Hewapathirana S, Kamatchinathan S, et al. The PRIDE database resources in 2022: a hub for mass spectrometry-based proteomics evidences. *Nucleic Acids Res.* 2022;50:D543–d52.

ACKNOWLEDGEMENTS

We gratefully acknowledge the use of the services and facilities of the Koç University Research Center for Translational Medicine (KUTTAM), funded by the Presidency of Turkey, Presidency of Strategy and Budget. We express sincere gratitude to William S. Saunders and Nicholas Quintyne for their intellectual contributions. Illustrations in the figures were created by using BioRender.com and licensed (AQ263P9YOS, XR263PAA8S, XL264EHWDK, JS263OX89L, TX263PBZZZ, LN263P92LT) for publication purposes.

AUTHOR CONTRIBUTIONS

Conceptualization: B.M.K. and C.A.A., Investigation: B.M.K., S.C.O., E.C. and M.G., Methodology: B.M.K. and S.C.O., Visualization: B.M.K., Project Administration: C.A.A., Funding Acquisition: C.A.A. and S.C.O., Writing—original draft: B.M.K. Writing—review & editing: C.A.A.

FUNDING

This study was funded by L’Oreal UNSECO (For Women in Science Award, 2018), BAGEP (Science Academy’s Young Scientist Awards Program, 2018), TUBA-GEBIP (Turkish Academy of Sciences- Outstanding Young Scientists Awards, 2017), TUBITAK 3501 Career Development Program (Grant no: 120Z830) and Eczacıbasi Scientific Research Support Awards (2019).

COMPETING INTERESTS

The authors declare no competing interests.

ETHICS APPROVAL AND CONSENT TO PARTICIPATE

Animal experiments were approved by Koç University Local Ethics Committee for Animal Experiments (HADYEK) with the protocol number 2023.HADYEK.046. No human subjects were included in the study.

ADDITIONAL INFORMATION

Supplementary information The online version contains supplementary material available at <https://doi.org/10.1038/s41419-024-06601-0>.

Correspondence and requests for materials should be addressed to Ceyda Acilan.

Reprints and permission information is available at <http://www.nature.com/reprints>

Publisher’s note Springer Nature remains neutral with regard to jurisdictional claims in published maps and institutional affiliations.



Open Access This article is licensed under a Creative Commons Attribution 4.0 International License, which permits use, sharing, adaptation, distribution and reproduction in any medium or format, as long as you give appropriate credit to the original author(s) and the source, provide a link to the Creative Commons licence, and indicate if changes were made. The images or other third party material in this article are included in the article’s Creative Commons licence, unless indicated otherwise in a credit line to the material. If material is not included in the article’s Creative Commons licence and your intended use is not permitted by statutory regulation or exceeds the permitted use, you will need to obtain permission directly from the copyright holder. To view a copy of this licence, visit <http://creativecommons.org/licenses/by/4.0/>.

© The Author(s) 2024